RESEARCH ARTICLE

Measuring the dynamic wind load acting on standing trees in the field without destroying them

Satoru Suzuki*, Ayana Miyashita

Center for Forest Damage and Risk Management, Forestry and Forest Products Research Institute, Tsukuba, Ibaraki, Japan

* satorusk@ffpri.affrc.go.jp

Abstract

Wind loads are a factor in tree growth, tree architecture, and the occurrence of disasters and forest disturbances, e.g., tree falls. To understand forest ecosystems and manage forests effectively, it is necessary to understand the relationship between wind loads and trees. However, wind speed and direction always vary, which makes it difficult to measure wind loads acting on trees dynamically. We have proposed a method to accurately measure the dynamic wind load (L_w), the centroid of the dynamic wind load distribution (C_L), and the dynamic wind load direction (D_L) using multiple strain gauges attached to a trunk. The advantage of this method is that it can quantify the moment by separating it into L_w and C_L. However, this method was only validated in a laboratory conditions by applying static loads to a cylinder pole and a small sapling. If this method can be applied to forest environments, it should provide meaningful results in areas such as forest ecology and forest conservation. Thus, in this study, the accuracy of measurement of these values was investigated under natural wind conditions to validate the feasibility of using the proposed method in a real-world field environment. At relatively higher wind speed, the accuracy of L_w was less than 10% of the systematic errors and the mean absolute percentage error (MAPE), the accuracy of C_L was less than 7.7% of the MAPE, and the accuracy of D_L was 12.3° of the mean absolute error (MAE). The influences of wind turbulence, the deformation of tree crown were also investigated. The results show that fluctuations in wind speed, wind direction, and the deformation have little effect on the accuracy of the values. The method employed in this study had sufficient characteristics to measure taller standing trees than the current sample in terms of sampling frequency. Thus, the method employed in this study can be widely used to measure dynamic L_w, C_L, and D_L of standing trees with the above accuracy in real-world field conditions.

OPEN ACCESS

Citation: Suzuki S, Miyashita A (2025) Measuring the dynamic wind load acting on standing trees in the field without destroying them. PLoS One 20(5): e0323532. https://doi.org/10.1371/journal.pone.0323532

Editor: Zeashan Hameed Khan, King Fahd University of Petroleum & Minerals, SAUDI ARABIA

Received: October 22, 2024

Accepted: April 9, 2025

Published: May 20, 2025

Data availability statement: All relevant data are available from the Figshare repository at the following DOI: https://doi.org/10.6084/m9.figshare.28237913.

Funding: This work is part of a research project "Improvement of risk evaluation for forest damage caused by meteorological factors based on

elucidation of the damage process." commissioned by the Forest Insurance Center of the Forestry and Forest Products Research Institute. The funders had no role in study design, data collection and analysis, decision to publish, or preparation of the manuscript.

Competing interests: The authors have declared that no competing interests exist.

Introduction

Both tree growth and survival are strongly related to wind loads; thus, it is necessary to measure the wind loads acting on trees to understand the morphogenesis of trees and forest ecosystems. For example, the ratio of trunk elongation to radial growth changes with loading. When trees are exposed to high winds or grown under forceful conditions that mimic high winds, elongation growth is suppressed, and hypertrophic growth is promoted [1]. Conversely, the opposite effect is observed when the trunk is fixed and allowed to grow in the absence of any force [2]. When the wind environment is regulated in wind tunnels and seedlings are grown, the root system growth is also affected. Lateral roots on the upwind and downwind sides, where the wind forces are primarily in effect, are thicker and longer [3]. Thus, both the aboveground and belowground parts of the tree grow in response to the wind loads to which they are exposed. The proposed principle for the effect of wind loading on growth is that each part of the trunk becomes enlarged, and the stress distribution in the trunk due to wind loading takes a particular form [4–6]. This hypothesis is convenient to relate trunk diameter to crown shape; however, it has not been fully verified as a mechanism for trunk formation [7], in part because wind loads cannot be measured directly.

In addition, wind loads are difficult to measure; thus, the magnitude of the wind loads and the mechanisms by which trees respond to wind loads are analyzed using both static and dynamic analysis techniques (sometimes in combination). The dynamic behavior of trees and the occurrence of damage are often assessed by estimating the moments acting on trees. For example, tree uprooting occurs when the moment applied by the wind load exceeds the strength of the root system, and snapping occurs when the stress on the trunk section exceeds the bending strength [8–10]. Several mechanical models, e.g., HWIND [11], GALES [12] and FOREOLE [13] have been developed based on this relationship. Moment is the product of the magnitude of the wind loads and the centroid of the wind load distribution. Therefore, by separately measuring the wind load and its centroid, it is possible to gain a deeper understanding of the physical phenomenon and to accurately estimate the moment.

In a previous study we proposed a method to measure the magnitude and direction of the wind load and the centroid of the wind load distribution acting on the tree using four strain gauges attached to the trunk of the tree[14]. The characteristics of this method are that it is possible to measure the moment by separating it into wind loads and centroid of wind loads, and that these can be measured with very high accuracy. However, the validity of the method was tested only for the samples subjected to static loading. To apply this method to forest trees, the measurement accuracy is required to be tested in natural wind environments where wind speed and direction vary over time.

In this study, our goal is to verify the accuracy of the proposed method regarding wind speed and the variation of wind speed/direction and to test the possibility of applying this method under field conditions. For this, we conducted the measurements of the magnitude, direction, and centroid of the wind load distribution acting on young Japanese ceder trees under natural wind conditions.

Materials and methods

Experimental design and apparatus

The study was conducted at the experimental field of the Forestry and Forest Products Research Institute (36°00′25″N, 140°7′37″E). The main wind direction at the study site was west, and there was no obstruction in the range of 20–90 m on a bearing from north to west, including the primary wind direction (Fig 1).

A 2–3 m section was cut from the top end of each of the sample trees, and four strain gauges were attached to the lower part of each trunk and placed on a six-axis load cell (LMC-61281, Nissho-Electric-Works, Tokyo, Japan) via a fixture (Fig 2). Three cedar trees (*Cryptomeria japonica*) were used for the measurements (Fig 3 and Table 1). The six-axis load

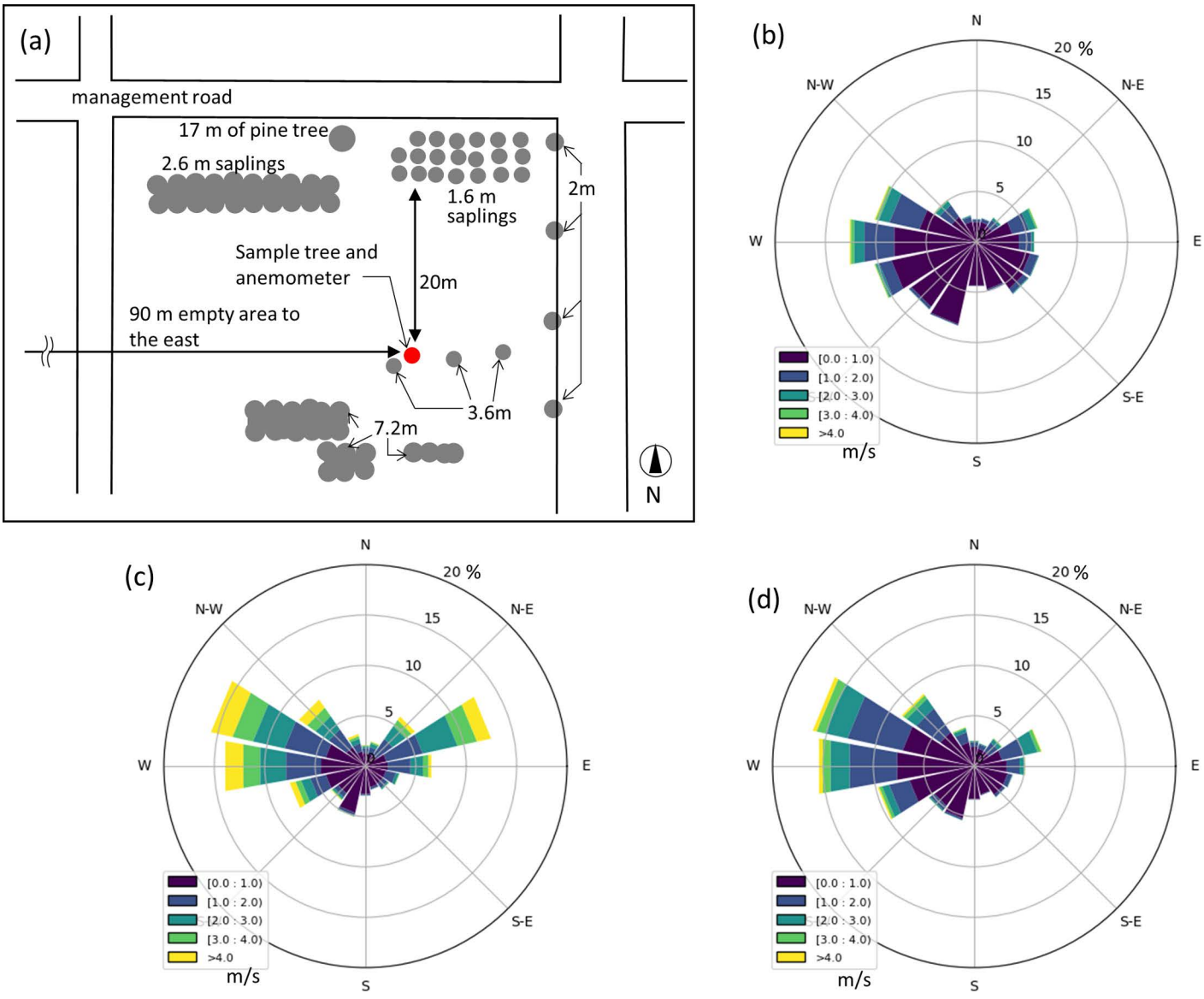

Fig 1. The arrangement of measurement location and surrounding trees (a), and the percentage of occurrences of wind speed and direction during the measurement period for Tree 1 (b), Tree 2 (c), and Tree 3 (d).

https://doi.org/10.1371/journal.pone.0323532.g001

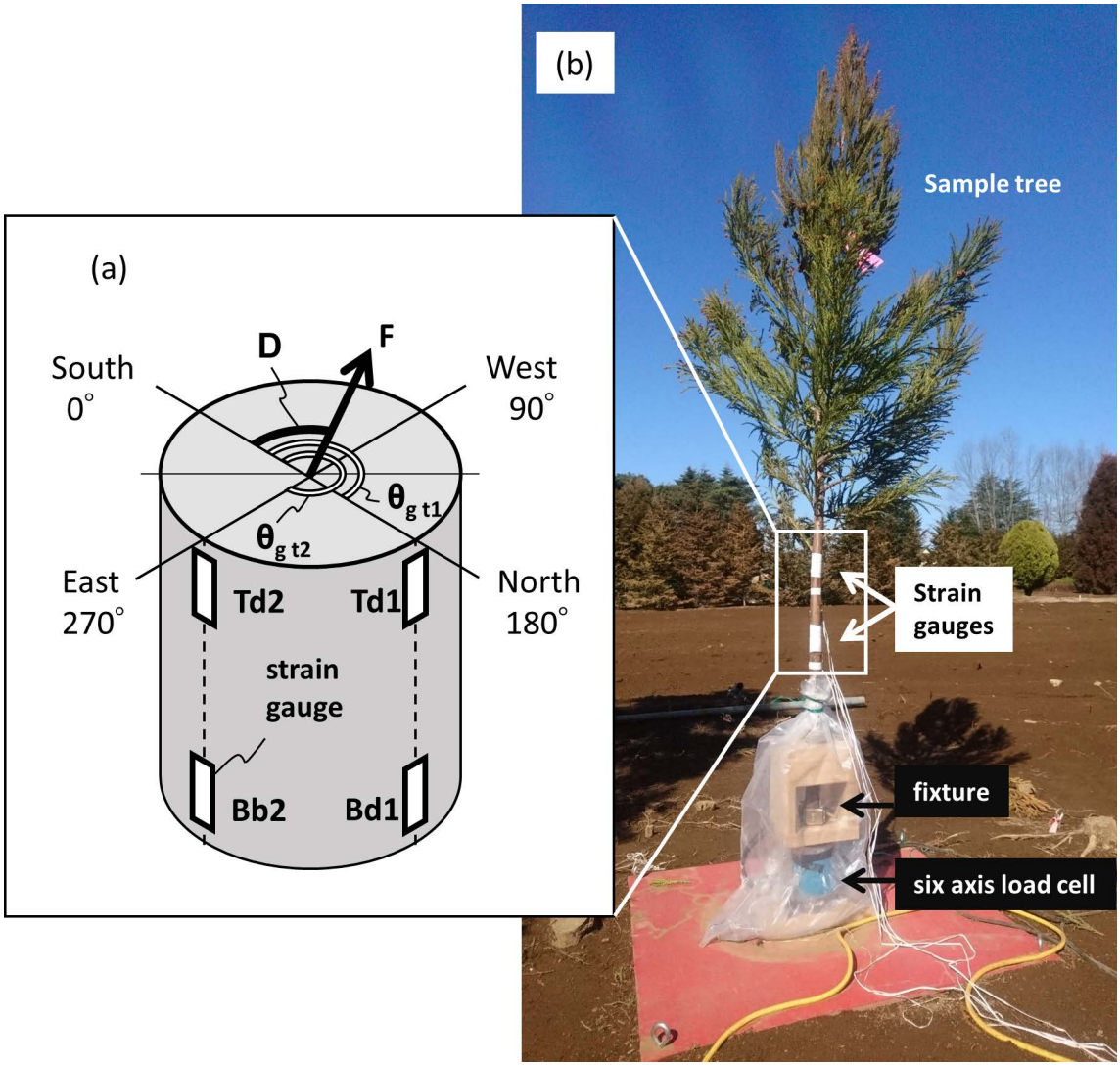

Fig 2. Diagrams of the arrangement of strain gauges and the experimental apparatus. Schema of the arrangement of strain gauges (a), fixing of sample tree (Tree 2) to load cell and arrangement of sensors (b) are shown.

https://doi.org/10.1371/journal.pone.0323532.g002

cell measures the loads and moments in the three orthogonal axes acting on the target object. To avoid exceeding the measurement limits of each component of moment, the height of the sample trees was limited to less than 3 m.

Strain gauges (KFRP-5-120-C1-1L5M3R, Kyowa Electronic, Tokyo, Japan) were attached using cyanoacrylate adhesive after removing the bark and the cambium layer from the trees. The strain gauges were attached to nearly orthogonal surfaces on the north and east sides of the trunks (the east and south sides for Tree 1). The strain gauge and six axis load cell readings were recorded at 10 Hz using a data logger (EDX-2000A, Kyowa Electronic, Tokyo, Japan). The measurement period for each sample tree was approximately one month. Note that this examination was conducted in winter, and cedar is relatively drought tolerant; thus the leaves remained green during the experiment period and no apparent changes were observed. The ultrasonic anemometer was fixed 3 m west of the sample trees at a height of 3 m. The three wind speed components were measured using an ultrasonic anemometer (CYG-81000, R.M. Young, MI, USA) and recorded on a data logger (CR3000X, Campbell, UT, USA) at 10 Hz.

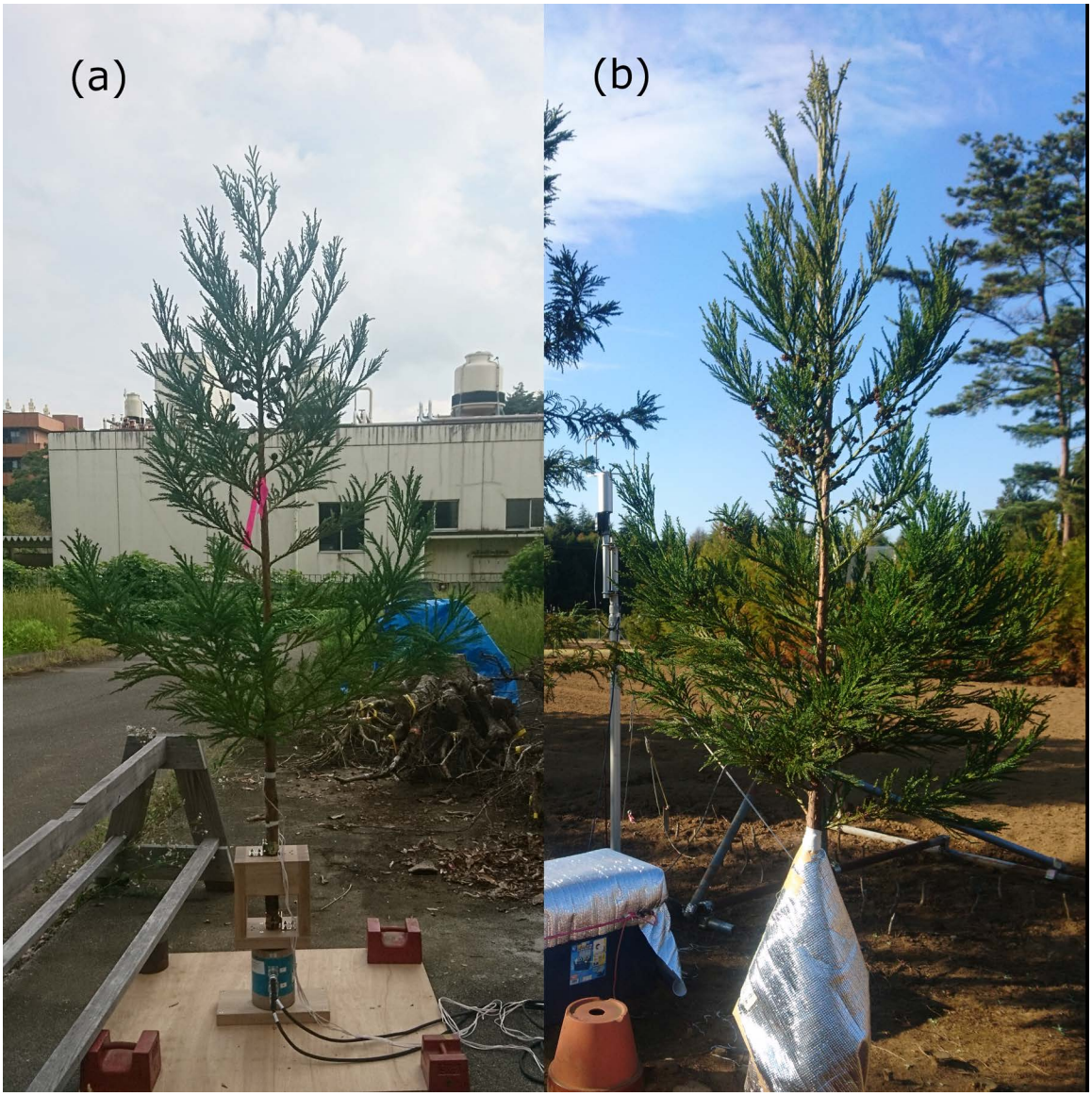

Fig 3. Photographs of the sample trees. Tree 1 (a) and Tree 3 (b) are shown. Tree 2 was shown in Fig 2b.

https://doi.org/10.1371/journal.pone.0323532.g003

Data from four days with high winds were analyzed (Table 2), and the analysis did not include the range where L_W was small due to low wind speed, i.e., $L_W < 1.0$ N and $L_{w\_ref} < 1.0$ N. Accuracy was verified by the mean absolute error (MAE) and mean absolute percentage error (MAPE) against the six-axis load cell readings. The natural frequencies of each sample tree were obtained from FFT analysis of the free vibration waveforms.

Calculating L_W, C_L and D_L

The magnitudes of the wind load (L_W), the height of the centroid of the distributed load (C_L), and the direction of the wind load (D_L) acting on the trees were calculated using a formulation of the technique presented by Miyashita and Suzuki [14]:

$$L_W = \frac{E_B \varepsilon_B Z_B - E_T \varepsilon_T Z_T}{(h_T - h_B)}, \tag{1}$$

Table 1. Sample trees.

Tree No.	Height (cm)	Center of gravity (cm)	Mass (kg)	Projected area* (m^2)	Diameter at gauges (cm)		Height at gauges (cm)		Natural Frequency (Hz)
					T	B	T	B	
1	205	89	2.4	0.84	3.0	3.2	45	32	1.5
2	233	119	3.3	0.70	3.1	3.4	67	47	0.9
3	286	131	4.9	1.34	3.4	3.7	65	41	0.8

* Projected area is the tree crown area projected onto a vertical plane.

https://doi.org/10.1371/journal.pone.0323532.t001

Table 2. Meteorological conditions on the day used for analysis. Data from the four days with the strongest wind speed during the measurement period were analysed. The measurements were taken at a height of 3m above the ground.

Tree No.	Date	Max. 10 min mean wind speed ($m\ s^{-1}$)	Max. wind speed measured at 10 Hz ($m\ s^{-1}$)	Daily mean air temperature (°C)
1	Oct. 20*	1.9	6.2	14.5
	Oct. 31	1.5	5.6	9.5
	Nov. 2	1.6	4.5	13.8
	Nov. 4	2.8	9.8	10.2
2	Mar. 6	2.5	8.0	11.9
	Mar. 10	4.2	13	9.3
	Mar. 13	3.8	11.6	11.1
	Mar. 14	4.6	15.7	11.1
3	Dec. 12	2.0	6.7	9.6
	Dec. 13	2.4	7.7	7.1
	Dec. 19	2.6	8.3	2.4
	Dec. 20	3.3	11.3	2.2

* data is available for half a day.

https://doi.org/10.1371/journal.pone.0323532.t002

$$C_L = \frac{E_T \varepsilon_T Z_T (h_T - h_B)}{E_B \varepsilon_B Z_B - E_T \varepsilon_T Z_T} + h_T, \tag{2}$$

$$D_L|_{T,B} = \left. arctan\left(\frac{\varepsilon_{d1} E_{d1} Z_{d1} \cos\theta_{gd2} - \varepsilon_{d2} E_{d2} Z_{d2} \cos\theta_{gd1}}{\varepsilon_{d2} E_{d2} Z_{d2} \sin\theta_{gd1} - \varepsilon_{d1} E_{d1} Z_{d1} \sin\theta_{gd2}} \right) \right|_{T,B.} \tag{3}$$

Here, ε, E, Z and h are the measured strain, Young's modulus, section modulus and height of the attached gauge, respectively, and the subscripts T and B indicate the upper and lower trunk locations, respectively. In addition, the subscripts d1 and d2 are the orientation on the attached trunk circumference (Fig 2). There are d1 and d2 strain gauges at each of the heights of T and B; thus, the direction of the wind load has two types of values calculated at T and B ($D_L|_T$ and $D_L|_B$). In this study, D_L was obtained as the vector direction that is a composite of the unit vectors in the $D_L|_T$ and $D_L|_B$ directions. Here, E_{d1}, E_{d2}, θ_{gd1}, and θ_{gd2} are the values obtained by a pulling test. Note that $Z_{d1}|_T = Z_{d2}|_T$ and $Z_{d1}|_B = Z_{d2}|_B$ were assumed in this study. A low-cut filter with a cutoff frequency of 0.0083 Hz (period of 120 s) was applied to ε_T and ε_B. To identify E and θ in Equation 1–3, pulling tests were performed during the measurement period for each sample tree (S1 File).

Obtaining the reference value using a six-axis load cell

The reference values for the wind load magnitude (L_{w_ref}), the centroid of the wind load distribution (C_{L_ref}), and the wind load direction (D_{L_ref}) were calculated using Equations (4–6) with a six-axis load cell:

$$L_{w\_ref} = \sqrt{F_x{}^2 + F_y{}^2} \tag{4}$$

$$C_{L\_ref} = \frac{\sqrt{M_x{}^2 + M_y{}^2}}{L_{w\_ref}}, \tag{5}$$

$$D_{L\_ref} = \arctan\left(\frac{F_y}{F_x}\right), \tag{6}$$

where F_x, F_y and M_x, and M_y are the loads and moments in two orthogonal directions in the horizontal plane, respectively. A low-cut filter with a cutoff frequency of 0.0083 Hz (period of 120 s) was applied to F_x, and F_y.

Identifying wind fluctuation and its properties

The degree of wind speed fluctuation was quantified by the turbulence intensity shown in Equation 7:

$$I = \frac{\sigma_U}{U_m} \tag{7}$$

where U_m and σ_U (m/s) are the mean and standard deviation of the wind speed for each 3 s period, respectively.

In addition to the magnitude of the wind direction, variability was quantified using a method defined by Yamartino [15], which is expressed as follows:

$$\sigma_{WD} = \arcsin(\delta)\left[1 + 0.1547\delta^3\right] . \tag{8}$$

Here,
σ_{WD} is the standard deviation over 3 s of the wind direction measured at 10 Hz, and δ is obtained as follows:

$$\delta = \sqrt{1 - \frac{1}{N^2}\left[\left\{\sum_i \left(\frac{U_{i\_x}}{U_i}\right)\right\}^2 + \left\{\sum_i \left(\frac{U_{i\_y}}{U_i}\right)\right\}^2\right]}. \tag{9}$$

Here, N is the number of data points, and U_{i_x} and U_{i_y} are the orthogonal wind velocity components of U_i measured at 10 Hz.

Calculating drag coefficients as an indicator of deformation and susceptibility to wind

Wind varies dynamically in terms of both speed and direction, and trees respond to wind loads like a smart structural system whose response varies with the magnitude of the load [16]. Typically, the magnitude of wind loads acting on trees is estimated by multiplying the square of the wind speed, the wind-receiving area, and the drag coefficient [11,17]. The drag coefficient is the factor used to convert the wind's velocity pressure into wind load acting on trees [18,19], and it is reflected by the degree of deformation of the tree crown [16,20] and the amount and presence of leaves[17]. Therefore, considering the drag coefficient as an indicator of deformation, we examined the relationship between the drag coefficient and measurement accuracy. The drag coefficient was calculated as follows:

$$C_d = \frac{2L_w}{\rho A U^2} \tag{10}$$

$$C_{d\_ref} = \frac{2L_{w\_ref}}{\rho A U^2} \tag{11}$$

where C_d is the drag coefficient for sample trees, C_{d_ref} is for reference. ρ is the air density. A is the sample tree's projected area on still-air (Table 1). U is wind speed.

Results

Comparison of 10-Hz measurement values with reference values

The time course of L_w and L_{w_ref} appeared to fluctuate in accordance with the variation of the wind speed (Fig 4a and c). In fact, L_w and L_{w_ref} increased with higher wind speed (Fig 6a, c and e) and the increasing rates of L_w and L_{w_ref} with wind speed were indicated with multipliers of 1.9, 1.9, and 1.4 for L_w, and multipliers of 1.8, 1.9, and 1.5 for L_{w_ref} from Trees 1–3, respectively, when regressed on a power function. The regression coefficients of L_w against L_{w_ref} for each sample tree were 1.00–1.07 (Fig 5a, d and g) and the coefficients of determination were greater than 0.94 for the linear regressions with an intercept of zero (Table 3).

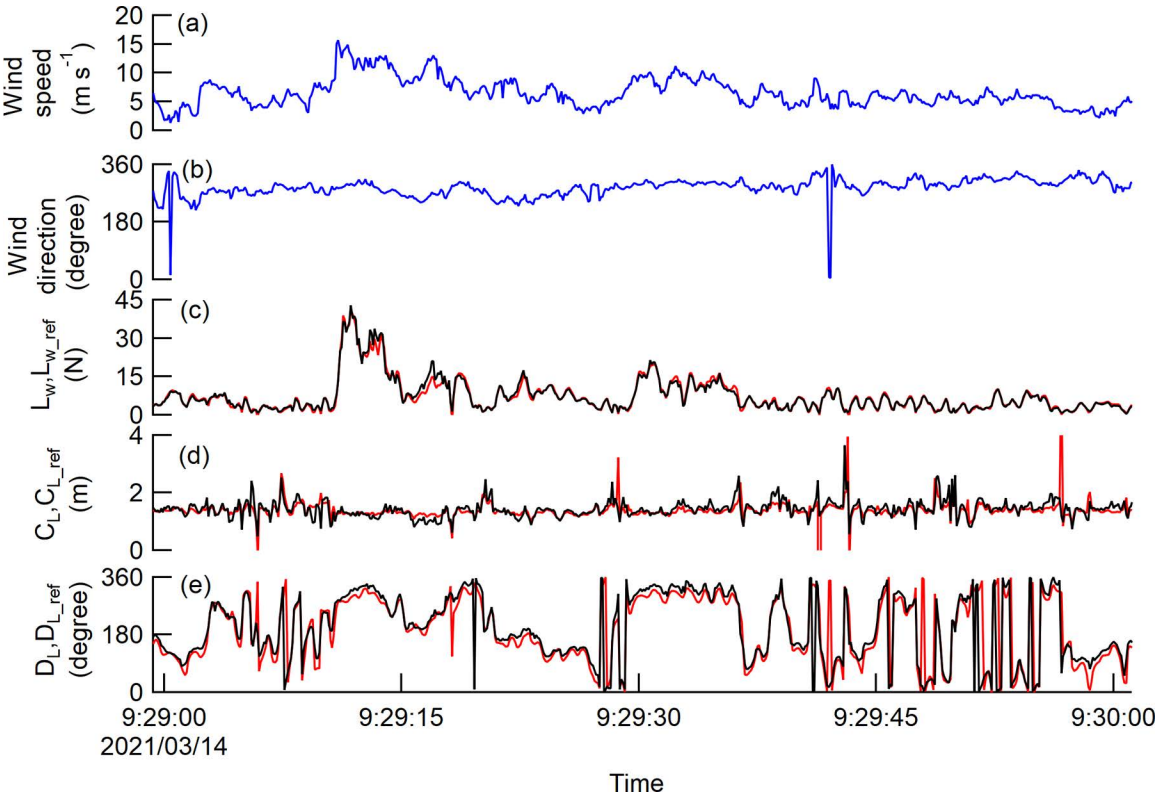

Fig 4. Time course of the values at 10-Hz measurement. The data were given for one minute from Tree 2, including the time at which the maximum wind speed was recorded. The time course of the wind speed (a) and the direction (b) are shown in blue lines. The red and black lines indicate the measured and reference values for graphs (c), (d), (e).

https://doi.org/10.1371/journal.pone.0323532.g004

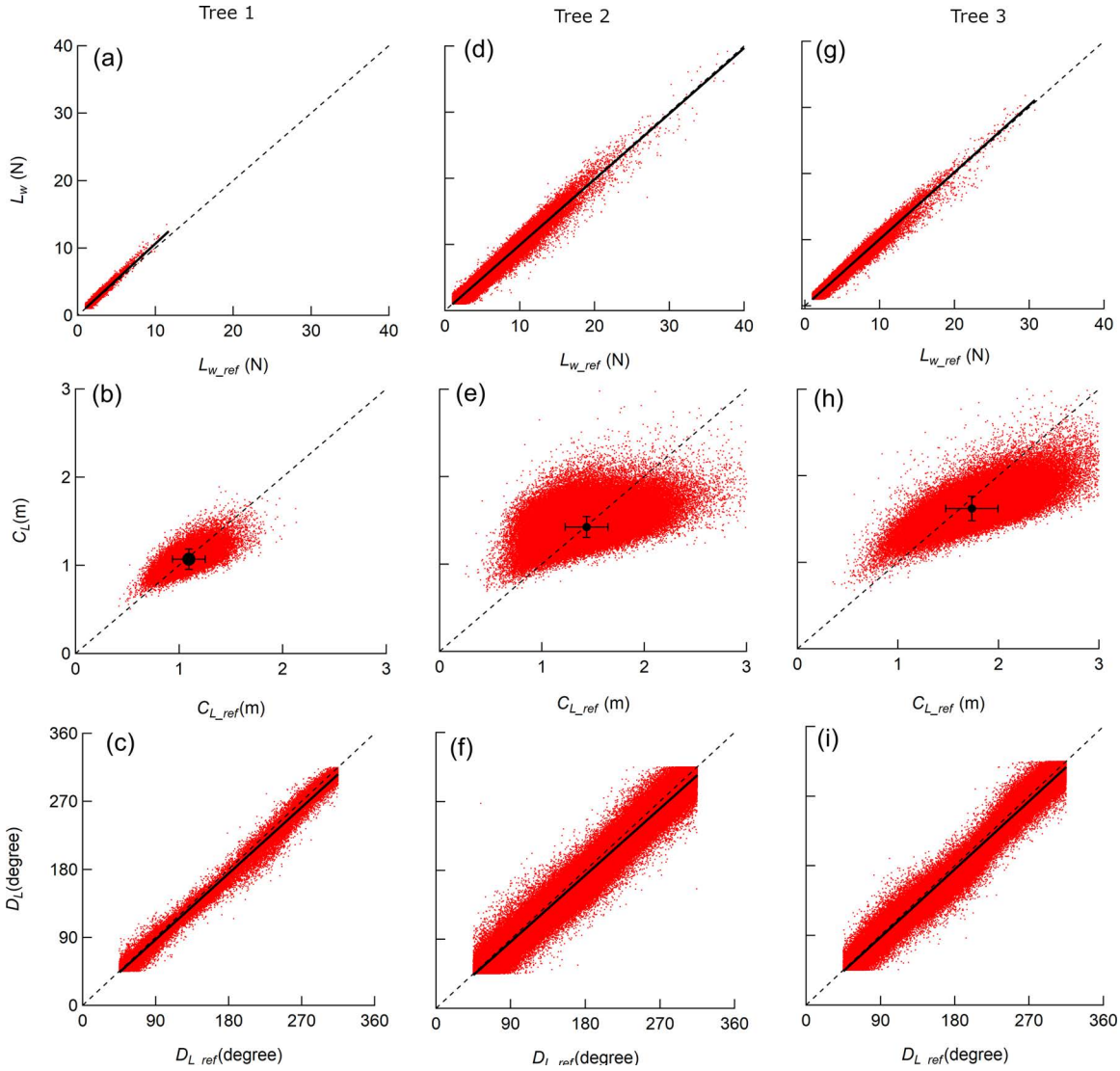

Fig 5. The measured values against the reference values at 10-Hz measurement. The measured and the reference values were obtained at 10 Hz for the wind load ((a), (d), (g)), the centroid of the distributed wind load ((b), (e), (h)), and the direction of the wind load ((c), (f), (i)) for each sample tree. Dashed line denotes 1:1 line. The dot and the error bars in (b), (e) and (h) denote mean value and the standard deviation.

https://doi.org/10.1371/journal.pone.0323532.g005

Although large amplitudes were occasionally seen for short periods of time, the time course of C_L and C_{L_ref} appeared to fluctuate around a certain value (Fig 4d). The fluctuation of the C_L and C_{L_ref} ranged from 0.8 m to the tree height. (Fig 5b, e and h). C_L tended to deviate from 1:1 as C_{L_ref} increased, and within the range, C_L was consistently smaller than C_{L_ref}. The class mean C_{L_ref} of Tree 3 showed a decrease of up to 0.2 m in response to an increase in wind speed, but for others, the range of fluctuation of the class mean C_L and C_{L_ref} was within 0.1 m and was almost constant regardless of wind speed (Fig 6b, d and f). The class mean C_L and C_{L_ref} closely matched for Tree 1 and 2 (Fig 6b and d), and the residuals of the mean C_L and the mean C_{L_ref} were 0.02 m for both the sample trees (Table 3). For Tree 3, the residuals of the mean C_L and the mean C_{L_ref} were relatively larger than other sample trees, with a value of 0.17 m (Table 3), but they were in good agreement at wind speeds of 6m/s or more (Fig 6f).

Table 3. Results related to the accuracy.

Tree No.	1	2	3	Overall
Regression coefficients of correlation between L_w vs L_{w_ref} (R^2)	1.07 (0.94)	1.00 (0.96)	1.06 (0.97)	-
Regression coefficients of correlation between D_L vs D_{L_ref} (R^2)	0.97 (0.98)	0.97 (0.98)	0.98 (0.98)	-
mean C_L, mean C_{L_ref} (m)	1.07, 1.09	1.42, 1.44	1.56, 1.73	-
sd C_L, sd C_{L_ref} (m)	0.12, 0.16	0.12, 0.21	0.12, 0.26	-
mean C_L/H, mean C_{L_ref}/H	0.51, 0.53	0.59, 0.60	0.54, 0.58	-
MAE_L (N)	0.18	0.30	0.27	0.28
$MAPE_L$ (%)	10.8	11.5	11.6	11.5
MAE_C (m)	0.09	0.15	0.22	0.17
$MAPE_C$ (%)	8.6	10.6	11.9	11.0
MAE_D (degrees)	8.6	10.4	8.6	9.6

MAE is the mean absolute error of [(1/n)Σ|(measured value)-(reference value)|]. MAPE is the mean absolute percentage error of [(100/n)Σ|{(measured value)-(reference value)}/(reference value)|]. The subscripts L, C, and D in MAE and MAPE indicate the wind load, the centoid of the distributed wind load, and the direction of the wind load. The overall values are calculated from all the sample trees. sd:standard deviation, H:tree height.

https://doi.org/10.1371/journal.pone.0323532.t003

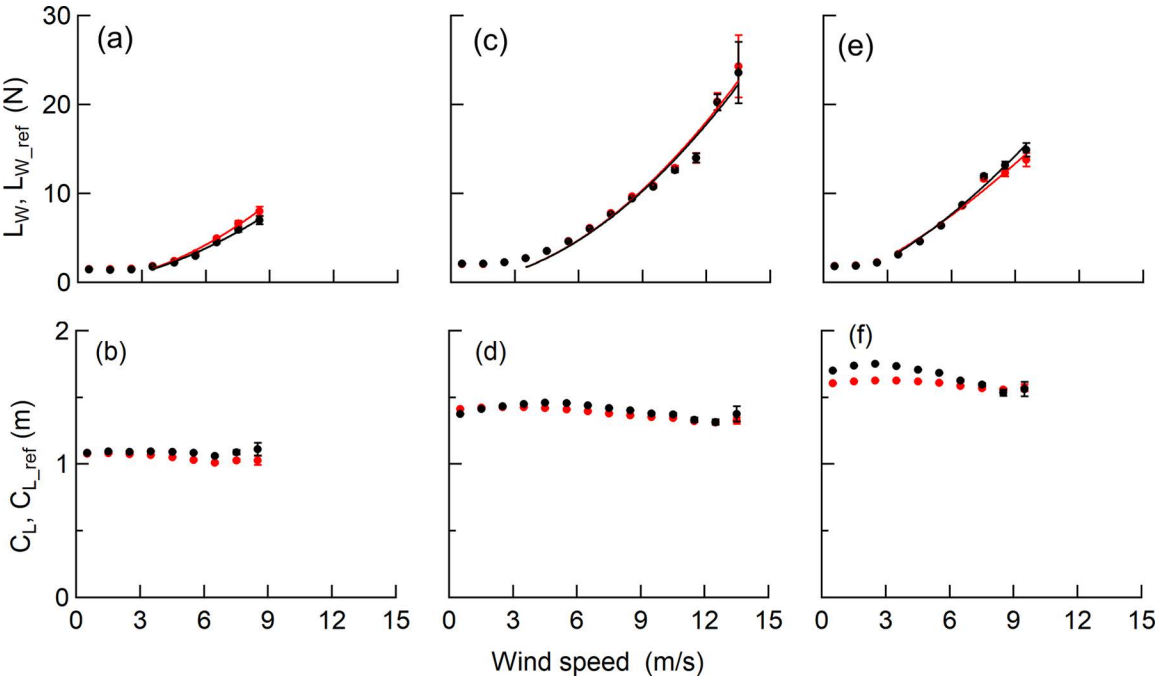

Fig 6. Comparison of 10-Hz measurement values for wind speed. The course of the class mean L_W, L_{w_ref} ((a), (c), (e)) and C_L, C_{L_ref} ((b), (d), (f)) are shown for each sample tree. These were obtained by averaging 10 Hz measurement values for wind speed classes. Error bars denote the standard error. Wind loads were regressed on a power function above 3 m/s with an intercept of zero as the analysis was carried out in L_W, L_{w_ref} > 1.0 N. Red circles and lines indicate the measured values. Black circles and lines indicate the reference values.

https://doi.org/10.1371/journal.pone.0323532.g006

The relationship between wind direction and the D_L, D_{L_ref} in the case shown in Fig 4 indicated that the wind direction remained almost constant at 270° over time (Fig 4b), but D_L and D_{L_ref} fluctuated with a large amplitude (Fig 4e). In terms of D_L against D_{L_ref}, we observed no apparent influence of the direction of the wind load as shown in the regression coefficient for each sample tree was greater than 0.97 (Fig 5c, f and i), and the coefficient of determination was greater than 0.98 for the linear regressions with an intercept of zero (Table 3).

Influence of wind speed on MAE and MAPE values

The MAE of L_W (MAE_L) for the wind speed class increased significantly with higher wind speed (Fig 7a). In contrast, the MAPE of L_W ($MAPE_L$) for the wind speed class indicated a significant decrease (Fig 7d). The MAE_L for each sample tree was 0.18–0.30 N, and the $MAPE_L$ for each sample tree was 10.8–11.6% (Table 3). To examine the overall trend, we calculated the MAE_L and $MAPE_L$ for all sample trees, and found that they were 0.28 N (SE = 0.0002 N, n = 1653456) of MAE_L and 11.5% (SE = 0.007%, n = 1653456) of $MAPE_L$ (Table 3).

Both the MAE of C_L (MAE_C) and MAPE of C_L ($MAPE_C$) for the wind speed class decreased with increasing wind speed, and the trends of the respective regression lines were significant (Fig 7b and e). The MAE_C values for each sample tree were 0.09–0.33 m, and the $MAPE_C$ values for each sample tree were 8.6–11.9% (Table 3). The overall MAE_C and $MAPE_C$ values for all sample trees to investigate the overall trend were 0.17 m (SE = 0.0001 m, n = 1653456) and 11.0% (SE = 0.007%, n = 1653456), respectively (Table 3).

The MAE of D_L (MAE_D) for the wind speed class increased with increasing wind speed, and the trend of the regression line was significant (Fig 7c). According to the regression line, the MAE_D value is expected to be 12° at the maximum wind

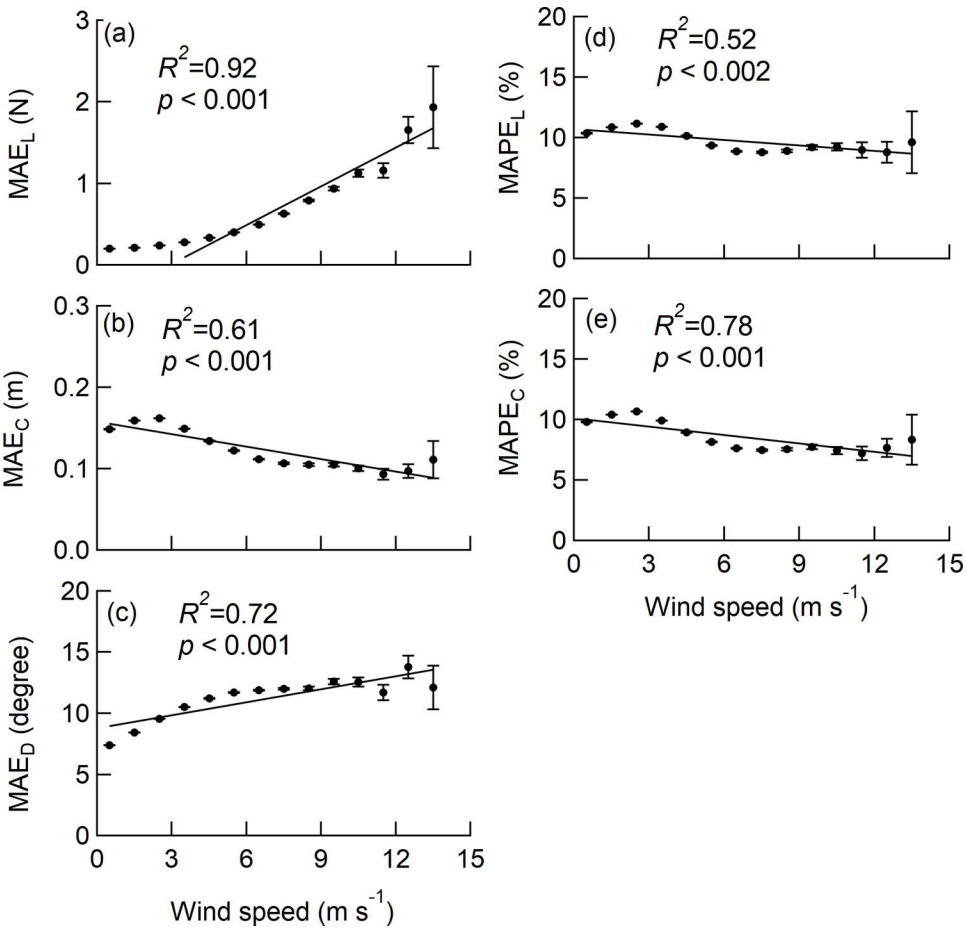

Fig 7. Influences of wind speed on the accuracy of L_W, C_L, and D_L. The class mean values were obtained from the values measured at 10 Hz for all sample trees. Since the MAPE of D_L cannot be defined, only the MAE_D is shown for D_L. Error bars denoted the standard error. The R^2 in the linear regression and the p value for the test on the regression coefficients are shown in the graphs. The significance of the regression coefficients was tested using a t-test.

https://doi.org/10.1371/journal.pone.0323532.g007

speed class. In addition,MAE_D values for each sample tree were 8.6–10.4° (Table 3). The overall MAE_D value for all sample trees to investigate the overall trend was 9.6° (SE = 0.006°, n = 1653456) (Table 3).

Influence of wind turbulence on L_W,C_L, and D_L measurements

The $MAPE_L$ value increased with increasing turbulence intensity and the standard deviation of the wind speed, and the observed trend was significant (Fig 8a and d); however, the coefficient of determination for the regression line was a low value ($R^2 = 0.36$) for turbulence intensity. The $MAPE_C$ value was nearly constant over the turbulence intensity, and the trend of the regression line for $MAPE_C$ was not significant (Fig 8b). The $MAPE_C$ value increased slightly as the standard deviation of the wind direction increased, and the trend of the regression line for $MAPE_L$ was significant (Fig 8e). The MAE_D value decreased slightly with increasing turbulence intensity, and the trend found to be significant (Fig 8c); however, the coefficient of determination for the regression line was low ($R^2 = 0.38$). In addition, the MAE_D value was nearly constant over the standard deviation of the wind direction, and the trend of the regression line for MAE_D was not significant (Fig 8f).

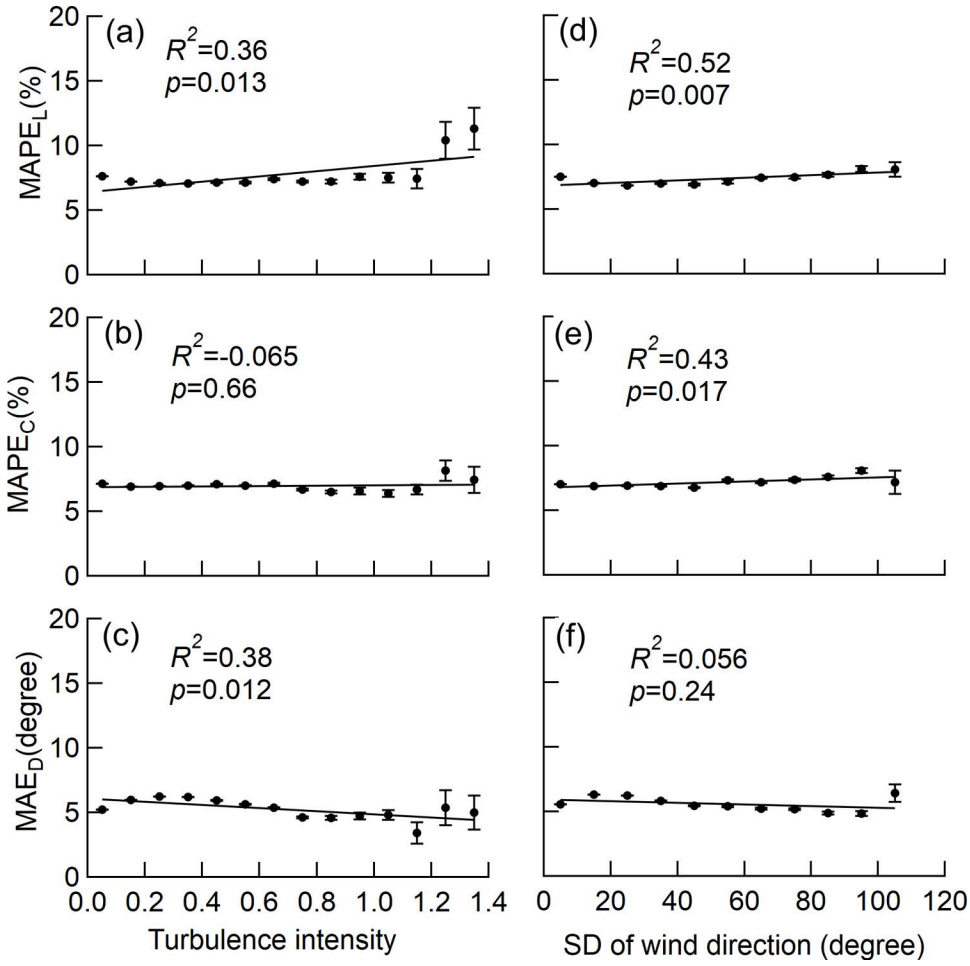

Fig 8. Influences of wind turbulence on the accuracy of L_W,C_L, and D_L. The class mean $MAPE_L$, $MAPE_C$ and MAE_D for the turbulent intensity of the wind speed ((a)-(c)), and the standard deviation of the wind direction ((d)-(f)) were shown. The values were obtained from all the sample trees with averaging 3 seconds readings. Error bars denoted the standard error. The R^2 in the linear regression and the p value for the test on the regression coefficients of $MAPE_L$, $MAPE_C$, and MAE_D are shown in the graphs. The significance of the regression coefficients was tested using a t-test.

https://doi.org/10.1371/journal.pone.0323532.g008

Influence of deformation on L_W, C_L, and D_L measurements

The drag coefficient decreased rapidly with increasing wind speed and became almost constant above a wind speed of 5 m/s, approaching asymptotically to 0.36 for both C_d and C_{d_ref} (Fig 9). This means that the C_d value decreases because the greater the wind speed, the greater the deformation of the crown to the wind. In addition, the deformation to the wind are considered to be almost constant at wind speeds of 5 m/s or more. The L_w showed a significant tendency for MAE and MAPE to decrease with decreasing drag coefficient (Fig 10a and d). The MAE_C and $MAPE_C$ had small coefficients of determination ($R^2 = 0.06$ for MAE_C, $R^2 = 0.36$ for $MAPE_C$) and the effect of the drag coefficient was considered to be negligible (Fig 10b and e). The MAE_D increased significantly with smaller drag coefficients significantly (Fig 10c).

Discussion

Measurement accuracy

Accuracy of L_w. As the wind speed increased, we found that L_w and L_{w_ref} increased rapidly, and the regression on the power function exhibited multipliers of 1.4–1.9 (Fig 6a, c and e). This indicates that the wind loads reflecting the wind pressure, which increases in proportion to the square of the wind speed, can be measured by using the method employed in the current study. As can be seen from Equations 10 and 11, as the drag coefficient decreases, the rate of increase of the wind load with respect to the increase in wind speed decreases. As the wind speed increased, the drag coefficient decreased (Fig 9), so that the multipliers were probably less than 2. The response of the drag coefficient to wind speed depends on the degree of deformation of the crown, and the multipliers likely reflect the characteristics of the response to the wind loading for each sample tree.

The results show opposite trends with wind speed: MAE_L increases while $MAPE_L$ decreases (Fig 7a and d). This is due to the fact that the increasing rate of L_{w_ref} with respect to the increase in wind speed exceeds the increasing rate of MAE_L, as is evident from the $MAPE_L$ formula. As the error of L_w decreased with increasing wind speed, $MAPE_L$ improved from

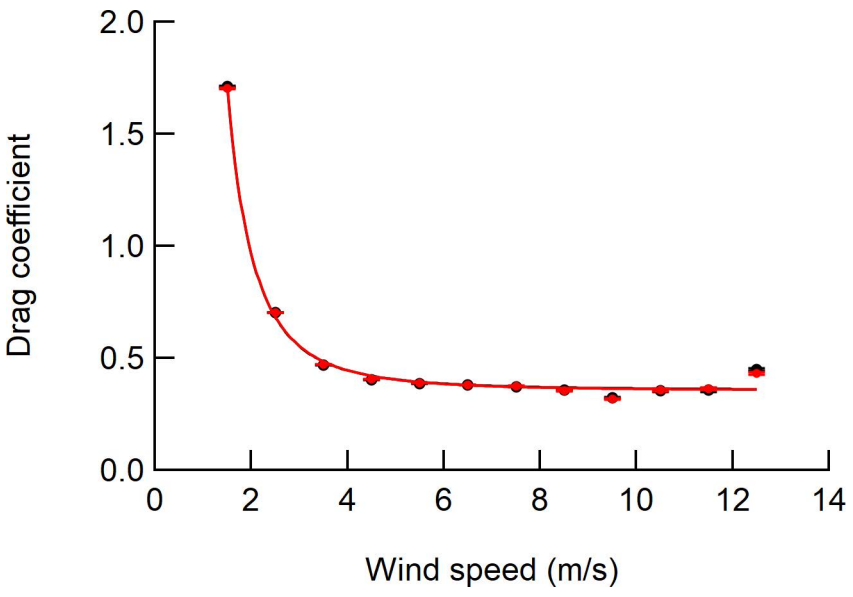

Fig 9. Influences of wind speed on the drag coefficient. The class mean drag coefficient for the wind speed was shown. The values were obtained by averaging 3 seconds readings. Error bars denote the standard error. Red circles and curves indicate the measured values. Black circles and curves indicate the reference values. The regression curve equation is $C_d = 0.36 + 4.14U^{-2.77}$ and $C_{d\_ref} = 0.36 + 4.21U^{-2.80}$.

https://doi.org/10.1371/journal.pone.0323532.g009

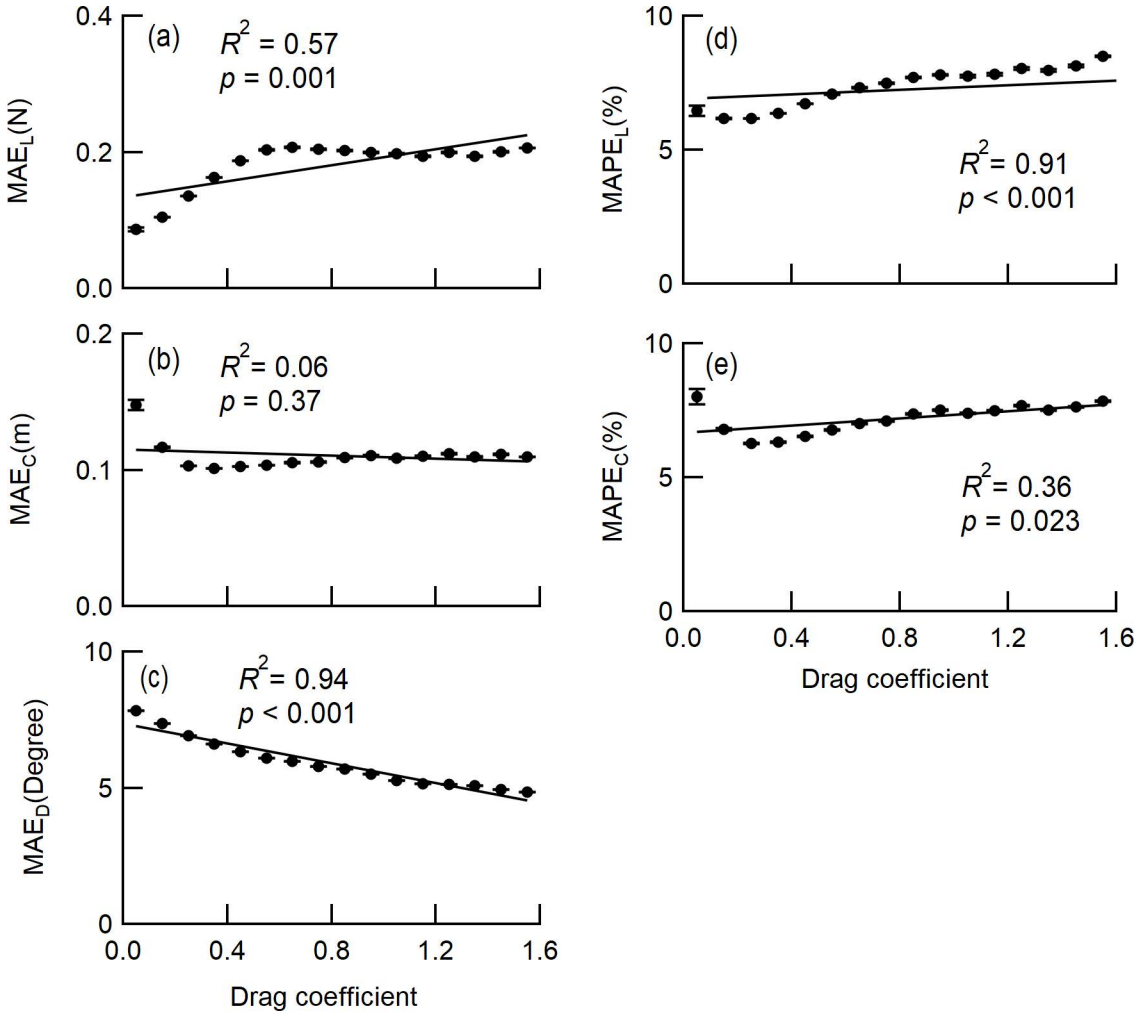

Fig 10. Influences of drag coefficient on the accuracy of L_w, C_L, and D_L. The class mean values were obtained by averaging 3-second readings. Since the MAPE of D_L cannot be defined, only the MAE$_D$ is shown for D_L. Error bars denote the standard error. The R^2 in the linear regression and the p value for the test on the regression coefficients are shown in the graphs. The significance of the regression coefficients was tested using a t-test.

https://doi.org/10.1371/journal.pone.0323532.g010

11.5% of the overall value to 9.1% in the higher wind speed range (wind speed >6 m/s) (Fig 7d). Since L_w is calculated from the difference in strain at the upper and lower positions (Eq. 1), higher wind speeds result in greater strain differences on the trunk; thus improving the accuracy of L_w. In addition, the accuracy of L_w, with regression coefficients for L_w and L_{w_ref} of 1.00–1.07, indicates that the systematic error is within 7% (Table 3).

In terms of the wind turbulence, the accuracy of L_w tended to worsen with increasing turbulence intensity and the standard deviation of wind direction, as demonstrated by the significant increase in MAPE$_L$ (Fis. 8a and 8d). However, the worsening of the MAPE$_L$ values was marginal, with only three points deterioration for the turbulence intensity and only one point deterioration for the standard deviation of wind speed over the observed range. In terms of wind turbulence, these results indicate that wind direction and fluctuations in wind speed, and the wind direction have little effect on the accuracy of the L_w measurements.

In terms of the drag coefficient, the fact that MAE$_L$ and MAPE$_L$ decrease when drag coefficient is small indicates that accuracy improves as the deformation is greater and less susceptibility to the wind. However, since the improvement in

MAE_L is 0.1N and the improvement in $MAPE_L$ is 1 point in the range of measurement, the effect of drag coefficient to the accuracy is thought to be small.

We usually make observations for the purpose of quantifying L_w, C_L, and D_L under relatively higher wind speed conditions. Thus, it can be concluded that the L_w measurements can be made practically with minimal influence from wind turbulence and deformation of the tree crown under real-world field conditions, with an accuracy of less than 10% of the systematic errors and the $MAPE_L$ in the range of higher wind speed.

Accuracy of C_L. The accuracy of the C_L tended to improve at higher wind speeds, as shown by the decrease in MAE_L and $MAPE_L$ value (Fig 7b and e). Since C_L is calculated using the difference in strain at the upper and lower positions (Eq. 2), higher wind speeds result in greater strain differences on the trunk, which in turn improves the accuracy of C_L. The improvement of accuracy was approximately 0.1 m in MAE_C and approximately 3 points in $MAPE_C$ over the observed wind speed range (Fig 7b and e). In addition, the accuracy at higher wind speeds (wind speed > 6 m/s) remained nearly constant, with an MAE_C of 0.1 m and an $MAPE_C$ of 7.7%.

In terms of wind turbulence, the magnitude of the fluctuations of wind speed did not influence the accuracy of C_L because the $MAPE_C$ value did not demonstrate a significant trend (Fig 8b). The increased fluctuations in wind direction tended to slightly worsen the accuracy of C_L, as demonstrated by the significant increase in the $MAPE_C$ value for the standard deviation of the wind direction (Fig 8e). However, the deterioration of the accuracy of C_L for wind direction fluctuation was marginal, showing only 1 point deterioration over the range of standard deviation of the wind direction. These results indicated that wind turbulence, as demonstrated by the fluctuations in wind speed and direction, has little effect on the accuracy of C_L measurements.

In terms of the drag coefficient, the determination coefficients for MAE_C and $MAPE_C$ were small, suggesting that the deformation and the susceptibility to the wind had little effect on the C_L measurement.

Thus, it can be concluded that C_L measurements could be made under real-world field conditions with an accuracy of approximately 0.17 m of MAE_C and 10.8% of $MAPE_C$ on average (Table 3), and even better accuracy was expected at higher wind speeds with an accuracy of approximately 0.10 m of MAE_C and 7.7% of $MAPE_C$.

Accuracy of D_L. Since D_L represents the direction in which the trunk has been displaced, its value depends on the position reflected by the trunk's sway and the wind load at a given moment. The sensitivity of a particular strain gauge is at maximum when the direction of the load is 180° or 0° against the sensitive direction of the gauge, and the minimum sensitivity is 0 when the direction of the load is 90° or 270°. There was a concern that the relationship between the strain gauges and the wind load direction may appear as the directionality of the D_L error. However, the directionality of the error was hardly observed because the regression coefficient of D_L against D_{L_ref} was greater than 0.97 with $R^2 > 0.98$ (Table 1). It has been reported that the accuracy was improved considerably by identifying the gauge mounting orientation and gauge sensitivity precisely by conducting pulling tests in multiple orientations [14]. The fact that relatively accurate D_L measurements were possible in this study regardless of the wind loading direction may be attributed to the fact that the pulling tests were performed in a similar manner.

The accuracy of D_L tended to worsen as the wind speed increased, as indicated by the significant increase in MAE_D (Fig 7c). In addition, the accuracy in the range of higher wind speed (wind speed > 6 m/s) looked nearly constant, with an MAE_D of 12.3°. The overall MAE_D for all sample trees was 9.6° at 10-Hz measurement.

In terms of wind turbulence, the accuracy of D_L tended to improve as the turbulence intensity of the wind speed, as demonstrated by the significant decrease in MAE_D (Fig 8c). However, the decrease in MAE_D estimated from the regression line was only 2° over the range of the turbulence intensity, and the coefficient of determination for the regression line was a low value ($R^2 = 0.36$). In addition, the MAE_D value did not trend significantly with the standard deviation of the wind direction (Fig 8f).

In terms of the drag coefficient, MAE_D increased as the drag coefficient decreased. This means that the measurement accuracy of D_L deteriorates due to deformation and less susceptibility to the wind. However, the deterioration was about 3 degrees in the range of measurement, so the effect was small.

Thus, it can be concluded that D_L measurements could be made under real-world field conditions with an accuracy of 9.6° of MAE_D on average, and it is expected that accuracy will deteriorate at higher wind speeds, with measurements taken with an accuracy of around 12.3°.

Accuracy comparison of laboratory and field measurements. In laboratory experiments, it has been reported that L_w and C_L could be measured within 4% of MAPE and D_L within 6° of MAE [14]. A possible reason for the larger error observed in the current study compared to the reported laboratory experiment is the difference in the reference. In the laboratory experiment, static loads with weights were used, whereas the reference utilized in the current study was based on the six-axis load cell measurements. The six-axis load cell has a certain amount of error, which means that the error in this study may be partially overestimated. In addition, we were unable to determine the cause of the tendency for C_L at 10 Hz to be smaller than the C_{Lref} value when the C_{L_ref} value is large (Fig 5b, e and h), but it may be due to the characteristics of the load cell used as the standard. The inability to set the pulling azimuth and elevation angle as precisely as in laboratory experiments when conducting pulling tests in the field is also considered to be a cause of the larger errors.

Advantages of the proposed approach

Nondestructive and dynamic measurement. In this study, we used a load cell to obtain the reference values. It may be reasonable to accept that using a load cell to measure the L_w, C_L, and D_L values would be sufficient. However, when using a load cell, it is necessary to cut the trunk and fix it on the instrument, which results in a limited measurement period to avoid degradation of the sample quality. The sizes of trees are also limited by the instrument's measurement capacity, and it is typically impossible to measure trees taller than only a few meters. In contrast, the method employed in the current study can be used by attaching strain gauges to the trunk of a standing tree without cutting it, and, in principle, there is no limit in terms of the size of the individual tree to be measured. The greatest advantage of the employed method is the ability to measure L_w, C_L, and D_L acting on a standing tree in a nearly nondestructive manner.

In the following, we discuss the applicability of this method to the size of the sample trees. The time resolution to be captured depends on the assumed phenomenon relative to the wind loads acting on the trees. An attempt has been made to estimate quasistatic wind loads as the mechanical loads affecting tree survival, based on the large frequency difference between the wind speed fluctuation and the sway of the tree [21]. However, frequency analyses of tree sway and wind speed fluctuations have indicated that the timing of gust onset coinciding with the sway corresponding to the direction of the gusts is important in terms of evaluating wind-induced tree falls [22]. It has also been observed that the forced swaying caused by a gust with a certain peak frequency in a typhoon caused trees to fall [23]. These findings imply that instantaneous wind loads are important in the evaluation of wind-induced tree falls. Tree sway responds to the fluctuations of wind load, and when measuring dynamic behavior, it is reasonable to focus the analysis on the first-order natural frequency of the sway [24]. To discretize the dynamic behavior of a tree with a first-order natural frequency (f_n), a sampling frequency (f_s) must be satisfied under the condition that $f_s > 2*f_n$ [25]. The maximum f_n of the sample trees observed in the current study was 1.5 Hz (Table 1); thus, the sampling frequency of 10 Hz employed in this study was sufficient to capture the dynamic behavior of the sample trees. In addition, the sampling frequency requirement to measure dynamic behavior is relaxed as the tree grows because the f_n of a tree decreases with increasing height [26]. Thus, the sampling frequency of 10 Hz employed in this study is valid even when measuring individual trees that are taller than the sample trees considered in this study. However, while the swaying of slender trees such as coniferous trees is governed by a single natural frequency, trees with large branch masses such as broad-leaved trees exhibit more complex swaying[27], so further research is needed to determine whether this method can be applied to trees with complex structures such as broad-leaved trees.

In addition, drag coefficients are frequently used to approximate loads, and gust factors are often used to approximate instantaneous loads. Such methods using coefficients are convenient ways to approximate loads. The method utilized in

the current study could also be useful to improve the accuracy of both drag coefficients and gust factors. In this study, we treated the drag coefficient as an indicator of deformation of crown and susceptibility to the wind, but the characteristics of the drag coefficient have been studied in various ways in the past, including its dependence on wind speed, projected canopy area, tree mass, canopy porosity, and the aeration of the canopy [18,19,28,29]. Generally, these characteristics have been investigated in uniform flow using a wind tunnel apparatus. However, the behavior of the drag coefficient in response to dynamic wind load fluctuations has not been fully clarified in field observations, such as the case where a large instantaneous drag coefficient [30] and large fluctuations in the drag coefficient due to tree swaying [17] were observed. The method employed in the current study is effective at elucidating the characteristics of the dynamic drag coefficient.

In terms of the gust factors, the instantaneous loads can be approximated by multiplying the gust factor by the mean loads. However, the gust factor of the wind load varies with the distance from the edge of the forest [31], and the gust factor of wind speed is affected by several factors, including surface roughness and atmospheric stability [32], which make it difficult to obtain accurate values. Using the method employed in this study, it should be possible to identify and characterize the gust factor because the mean and instantaneous load values can be obtained easily.

Centroid quantification. Recently, the response of trees has been analyzed dynamically, including examining the relationship between the structure of tree stem, branches, and leaves and the swaying of individual trees[33,34], and examining the collisions between individual trees caused by swaying and the stability of individual trees[23]. In these studies, the sway was measured using various devices, including prisms [35], inclinometers [21,36,37], extensometers[17], displacement transducers [38], strain gauges [26,39] and accelerometers [40,41]. There have been attempts to estimate the dynamic variation of moments by multiplying the sensor readings by a coefficient that expresses the relationship between the tree motion and the moment [39,42,43]. However, in all of these devices, it is not possible to quantify the wind load and the centroid of wind load separately. In other words, another feature of our method is that it is possible to quantify the moment by separating it into wind load and centroid.

The height of the centroid is frequently given as the centroid of the projected area of the tree crown to the vertical plane [17,44]. This assumes that the wind has uniform velocity pressure across the projected area of the canopy, i.e., a uniform flow is present, and that the drag coefficient is spatially uniform. Thus, the further away the wind speed distribution is from uniform flow, or the more heterogeneous the spatial distribution of the drag coefficient is, the further it is from the centroid of the projected area. This affects the calculation of wind loads and moments acting on the individual tree.

Based on photographs, the centroid of the projected area of the crown to the vertical plane (relative height of the centroid to the tree height) was calculated, and the values for Trees 1–3 were 1.15 m (0.56), 1.55 m (0.66), and 1.64 m (0.57), respectively, and these values were up to 9% greater than C_L and C_{L_ref} values.

To calculate the moment, C_L and C_{L_ref} values are multiplied by L_w, and the critical wind speed is calculated as the wind speed that balances the moment with the resistive strength of the root system and the bending strength of the trunk [11]. Assuming that the centroid is overestimated by 9%, and L_w is calculated accurately, the critical wind speed is estimated to be 4.2% lower than the true value. Generally, the critical wind speeds range 10–40 m/s [9,11,13,45]. Therefore, the critical wind speed will be underestimated by 0.4–1.7 m/s. In this study, the difference between the centroid from the tree shape and from C_L and C_{L_ref} was small because there were open areas near the main wind direction, and the vertical wind speed distribution in the canopy was relatively uniform. However, the C_L value may deviate significantly from the centroid of the projected area of the tree canopy when there is a significant vertical distribution of wind speed, and the distribution of branches and leaves is not spatially uniform, such as in a forest environment. Although the centroid is an important factor in terms of estimating the moments acting on the tree, there are few cases where it has been measured. The method employed in the current study could be used to elucidate the relationship between forest conditions and the mechanical processes that convert wind energy into moment.

Conclusions

Both tree growth and survival are strongly related to wind loads; thus, development of a technique to measure wind loads acting on trees can provide a technical basis to understand tree morphogenesis and forest ecosystems. In this study, the magnitude, direction, and centroid of the wind load distribution acting on trees were measured under natural wind conditions using a previously proposed method [14]. We verified the accuracy of the method regarding wind speed and the variation of wind speed/direction and considered the possibility of applying this method under real-world field conditions. Our findings are summarized as follows:

(i) The wind load (L_w) measurements can be performed practically with minor influences of wind turbulence and tree deformation under real-world field conditions, with an accuracy of less than 10% of the systematic errors and the MAPE in the range of higher wind speed of more than 6 m/s.

(ii) The centroid of the wind load distribution (C_L) measurements could be made under real-world field conditions with an accuracy of approximately 0.17 m of MAE and 10.8% of MAPE on average; even better accuracy can be expected at higher wind speeds with an accuracy of approximately 0.10 m of MAE and 7.7% of MAPE.

(iii) The wind load direction (D_L) measurements could be made under real-world field conditions with an accuracy of 9.6° of MAE on average, but it was predicted that the accuracy would decrease at higher wind speeds with an accuracy of approximately 12.3°.

(iv) The method employed in this study had sufficient characteristics to measure higher standing trees than the current sample (2–3 m of tree height) in terms of sampling frequency.

Thus, the method employed in this study can be widely used to measure dynamic L_w, C_L, and D_L of standing trees with the above accuracy.

Supporting information

S1 File. The procedures of pulling test and the apparent value of the modulus of elasticity and the radial position of each strain gauge, and the accuracy using determined parameters.
(DOCX)

Acknowledgements

We sincerely thank Dr. Kenjiro Hayashi for valuable discussions and technical instruction.

Author contributions

Conceptualization: Satoru Suzuki.

Data curation: Ayana Miyashita.

Formal analysis: Satoru Suzuki, Ayana Miyashita.

Funding acquisition: Satoru Suzuki.

Investigation: Satoru Suzuki, Ayana Miyashita.

Methodology: Satoru Suzuki, Ayana Miyashita.

Project administration: Satoru Suzuki.

Software: Satoru Suzuki, Ayana Miyashita.

Supervision: Satoru Suzuki.

Validation: Ayana Miyashita.

Writing – original draft: Satoru Suzuki.

Writing – review & editing: Ayana Miyashita.

References

1. Pruyn ML, Ewers III BJ, Telewski FW. Thigmomorphogenesis: changes in the morphology and mechanical properties of two Populus hybrids in response to mechanical perturbation. Tree Physiol. 2000;20(8):535–40. https://doi.org/10.1093/treephys/20.8.535 PMID: 12651434
2. Holbrook NM, Putz FE. Influence of neighbors on tree form: effects of lateral shade and prevention of sway on the allometry of Liquidambar Styraciflua (sweet gum). Am J Bot. 1989;76(12):1740–9. https://doi.org/10.1002/j.1537-2197.1989.tb15164.x
3. Tamasi E, Stokes A, Lasserre B, Danjon F, Berthier S, Fourcaud T, et al. Influence of wind loading on root system development and architecture in oak (*Quercus robur L.*) seedlings. Trees. 2005;19(4):374–84. https://doi.org/10.1007/s00468-004-0396-x
4. Dean TJ, Roberts SD, Gilmore DW, Maguire DA, Long JN, O'Hara KL, et al. An evaluation of the uniform stress hypothesis based on stem geometry in selected North American conifers. Trees. 2002;16(8):559–68. https://doi.org/10.1007/s00468-002-0208-0
5. Mattheck C, Bethge K. The structural optimization of trees. Naturwissenschaften. 1998;85(1):1–10. https://doi.org/10.1007/s001140050443
6. Meng SX, Lieffers VJ, Huang S. Modeling crown volume of lodgepole pine based upon the uniform stress theory. For Ecol Manag. 2007;251(3):174–81. https://doi.org/10.1016/j.foreco.2007.06.008
7. Clair B, Fournier M, Prevost MF, Beauchene J, Bardet S. Biomechanics of buttressed trees: bending strains and stresses. Am J Bot. 2003;90(9):1349–56. https://doi.org/10.3732/ajb.90.9.1349 PMID: 21659235
8. Achim A, Ruel J-C, Gardiner BA. Evaluating the effect of precommercial thinning on the resistance of balsam fir to windthrow through experimentation, modelling, and development of simple indices. Can J For Res. 2005;35(8):1844–53. https://doi.org/10.1139/x05-130
9. Achim A, Ruel J-C, Gardiner BA, Laflamme G, Meunier S. Modelling the vulnerability of balsam fir forests to wind damage. For Ecol Manag. 2005;204(1):37–52. https://doi.org/10.1016/j.foreco.2004.07.072
10. Hale SE, Levy PE, Gardiner BA. Trade-offs between seedling growth, thinning and stand stability in Sitka spruce stands: a modelling analysis. For Ecol Manag. 2004;187(1):105–15. https://doi.org/10.1016/s0378-1127(03)00313-x
11. Peltola H, Kellomäki S, Väisänen H, Ikonen V-P. A mechanistic model for assessing the risk of wind and snow damage to single trees and stands of Scots pine, Norway spruce, and birch. Can J For Res. 1999;29(6):647–61. https://doi.org/10.1139/x99-029
12. Gardiner B, Peltola H, Kellomäki S. Comparison of two models for predicting the critical wind speeds required to damage coniferous trees. Ecol Modell. 2000;129(1):1–23. https://doi.org/10.1016/s0304-3800(00)00220-9
13. Ancelin P, Courbaud B, Fourcaud T. Development of an individual tree-based mechanical model to predict wind damage within forest stands. For Ecol Manag. 2004;203(1–3):101–21. https://doi.org/10.1016/j.foreco.2004.07.067
14. Miyashita A, Suzuki S. A method for measuring the forces acting on a tree trunk using strain gauges. PLoS One. 2021;16(1):e0245631. https://doi.org/10.1371/journal.pone.0245631 PMID: 33449960
15. Yamartino RJ. A Comparison of Several "Single-Pass" estimators of the standard deviation of wind direction. J Climate Appl Meteor. 1984;23(9):1362–6. https://doi.org/10.1175/1520-0450(1984)023<1362:acospe>2.0.co;2
16. Ishikawa H, Amano S, Yakushiji K. Flow around a living tree. JSME Int J Ser B. 2006;49(2):1064–9.
17. Koizumi A, Motoyama J, Sawata K, Sasaki Y, Hirai T. Evaluation of drag coefficients of poplar-tree crowns by a field test method. J Wood Sci. 2010;56(3):189–93. https://doi.org/10.1007/s10086-009-1091-8
18. Mayhead GJ. Some drag coefficients for British forest trees derived from wind tunnel studies. Agric Meteorol. 1973;12:123–30. https://doi.org/10.1016/0002-1571(73)90013-7
19. Rudnicki M, Mitchell SJ, Novak MD. Wind tunnel measurements of crown streamlining and drag relationships for three conifer species. Can J For Res. 2004;34(3):666–76. https://doi.org/10.1139/x03-233
20. Vollsinger S, Mitchell SJ, Byrne KE, Novak MD, Rudnicki M. Wind tunnel measurements of crown streamlining and drag relationships for several hardwood species. Can J For Res. 2005;35(5):1238–49. https://doi.org/10.1139/x05-051
21. Kolbe S, Rentschler F, Frey J, Seifert T, Gardiner B, Detter A, et al. Assessment of effective wind loads on individual plantation-grown forest trees. Forests. 2022;13(7):1026. https://doi.org/10.3390/f13071026
22. Gardiner BA. The interactions of wind and tree movement in forest canopies. In: Coutts MP, Grace J, editors. Wind and trees. Cambridge: Cambridge university press; 1995. p. 485.
23. Kamimura K, Nanko K, Matsumoto A, Ueno S, Gardiner J, Gardiner B. Tree dynamic response and survival in a category-5 tropical cyclone: the case of super typhoon Trami. Sci Adv. 2022;8(10):eabm7891. https://doi.org/10.1126/sciadv.abm7891 PMID: 35275731
24. Sellier D, Fourcaud T, Lac P. A finite element model for investigating effects of aerial architecture on tree oscillations. Tree Physiol. 2006;26(6):799–806. https://doi.org/10.1093/treephys/26.6.799 PMID: 16510396

25. Brandt A. Noise and vibration analysis: signal analysis and experimental procedures. John Wiley & Sons, Ltd. 2011. p. 35–61.
26. Moore JR, Maguire DA. Natural sway frequencies and damping ratios of trees: influence of crown structure. Trees. 2004;19(4):363–73. https://doi.org/10.1007/s00468-004-0387-y
27. Jackson T, Shenkin A, Moore J, Bunce A, van Emmerik T, Kane B, et al. An architectural understanding of natural sway frequencies in trees. J R Soc Interface. 2019;16(155):20190116. https://doi.org/10.1098/rsif.2019.0116 PMID: 31164076
28. Grant PF, Nickling WG. Direct field measurement of wind drag on vegetation for application to windbreak design and modelling. Land Degrad Dev. 1998;9(1):57–66. https://doi.org/10.1002/(sici)1099-145x(199801/02)9:1<57::aid-ldr288>3.0.co;2-7
29. Cao J, Tamura Y, Yoshida A. Wind tunnel study on aerodynamic characteristics of shrubby specimens of three tree species. Urban For Urban Green. 2012;11(4):465–76. https://doi.org/10.1016/j.ufug.2012.05.003
30. Shiigai H, Maruyama T. Measurement of wind drag forces on trees. Nat Disast Sci. 1988;10(2):25–33.
31. Gardiner BA, Stacey GR, Belcher RE, Wood CJ. Field and wind tunnel assessments of the implications of respacing and thinning for tree stability. Forestry. 1997;70(3):233–52. https://doi.org/10.1093/forestry/70.3.233
32. Verkaik JW. Evaluation of two gustiness models for exposure correction calculations. J Appl Meteor. 2000;39(9):1613–26. https://doi.org/10.1175/1520-0450(2000)039<1613:eotgmf>2.0.co;2
33. Kamimura K, Nanko K, Matsumoto A, Ueno S, Gardiner B. Energy transfer during tree movement for different wind conditions and forest configurations. For Ecol Manag. 2024;571:122223. https://doi.org/10.1016/j.foreco.2024.122223
34. James KR, Haritos N, Ades PK. Mechanical stability of trees under dynamic loads. Am J Bot. 2006;93(10):1522–30. https://doi.org/10.3732/ajb.93.10.1522 PMID: 21642099
35. Hassinen A, Lemettinen M, Peltola H, Kellomäki S, Gardiner B. A prism-based system for monitoring the swaying of trees under wind loading. Agric For Meteorol. 1998;90(3):187–94. https://doi.org/10.1016/s0168-1923(98)00052-5
36. Dupont S, Défossez P, Bonnefond J-M, Irvine MR, Garrigou D. How stand tree motion impacts wind dynamics during windstorms. Agric For Meteorol. 2018;262:42–58. https://doi.org/10.1016/j.agrformet.2018.06.022
37. Schindler D, Mohr M. No resonant response of Scots pine trees to wind excitation. Agric For Meteorol. 2019;265:227–44. https://doi.org/10.1016/j.agrformet.2018.11.021
38. Milne R. Dynamics of swaying of Picea sitchensis. Tree Physiol. 1991;9(3):383–99. https://doi.org/10.1093/treephys/9.3.383 PMID: 14972849
39. Duperat M, Gardiner B, Ruel J-C. Effects of a selective thinning on wind loading in a naturally regenerated balsam fir stand. For Ecol Manag. 2022;505:119878. https://doi.org/10.1016/j.foreco.2021.119878
40. Peltola H. Swaying of trees in response to wind and thinning in a stand of Scots pine. Boundary-Layer Meteorol. 1996;77(3–4):285–304. https://doi.org/10.1007/bf00123529
41. van Emmerik T, Steele-Dunne S, Hut R, Gentine P, Guerin M, Oliveira RS, et al. Measuring tree properties and responses using low-cost accelerometers. Sensors (Basel). 2017;17(5):1098. https://doi.org/10.3390/s17051098 PMID: 28492477
42. Duperat M, Gardiner B, Ruel J-C. Testing an individual tree wind damage risk model in a naturally regenerated balsam fir stand: potential impact of thinning on the level of risk. Forestry. 2020;94(1):141–50. https://doi.org/10.1093/forestry/cpaa023
43. Wellpott A. The stability of continuous cover forests. University of Edinburgh; 2008.
44. Kane B, Smiley ET. Drag coefficients and crown area estimation of red maple. Can J For Res. 2006;36(8):1951–8. https://doi.org/10.1139/x06-086
45. Dupont S, Pivato D, Brunet Y. Wind damage propagation in forests. Agric For Meteorol. 2015;214–215:243–51. https://doi.org/10.1016/j.agrformet.2015.07.010